INFORMATION THEORETIC BOUNDS ON SOURCE LOCALIZATION PERFORMANCE

John R. Buck

University of Massachusetts Dartmouth
ECE Department and School of Marine Science and Technology
285 Old Westport Road
North Dartmouth, MA 02747

ABSTRACT

This paper examines the underwater acoustic source localization problem as an unorthodox communication problem. This perspective produces novel bounds on the performance of any source localization algorithm. The search space is divided into a grid whose cell size is determined by operational constraints. The message transmitted by the source is the cell it is located within. The receiver uses pressure observations from a sensor array to receive this message with a minimum probability of error. A necessary condition to choose the correct grid cell with arbitrarily small positive probability of error is that the mutual information between the source location and the estimate of it must equal or exceed the entropy of the grid. This mutual information can be bounded from above using the Gaussian channel approximation. The source channel coding theorem then determines the minimum necessary SNR to achieve a desired range resolution, or equivalently the best possible range resolution for a given SNR, assuming arbitrarily small probability of error. The resulting resolution bound is discussed in comparison to the Cramer-Rao Bound. The resolution bound is computed for typical underwater environments, and Monte-Carlo experiments are presented for these same environments.

1. INTRODUCTION

Underwater source localization (SL) estimates the position of an unknown source from the pressure observed at an array of hydrophones. This paper focuses on the scenario where the source emits a single narrowband tone at frequency f and is stationary over the observation interval. The search space will be a 2D range-depth (r, z) plane, though the results are easily extended to include bearing.

The traditional approach to SL is estimation theory. The location is considered an unknown parameter to be estimated in an (ideally) unbiased manner with minimum variance. Both beamforming [1][2] and matched field processing (MFP) [3] are examples of this approach. The maximum likelihood estimator for this problem and Cramer-Rao lower bound (CRLB) on the variance of the source location were derived in [4]. Subsequent investigations found that the height of the sidelobes in the ambiguity plane rather than the sharpness of the mainlobe limited the performance of MFP for the low SNR typical for underwater SL. The CRLB is based on the local curvature of the probability density function (pdf) as a function of source location, and thus may incompletely represent the factors limiting performance in these low SNR scenarios.

Information theory provides an alternative perspective on the problem. Consider dividing the search space of possible source locations into a grid of $\ell = 1, 2, \ldots, L$ cells as shown in Fig. 1. The source may be anywhere within a range interval of R and a depth interval of Z. In many practical scenarios, it is sufficient to locate the source within a grid cell of width Δr and to classify it as a surface or submerged source depending on whether it is shallower or deeper than some depth z_0. Rough nominal values for a typical shallow water problem might be $R = 10$ km, $\Delta r = 200$–300 m, z_0 = 20 m, and $Z = 100$ m. The grid covering this interval would have at most 100 cells, and if all cells are equally likely, the source location will take at most $\log_2(100) \approx 6.6$ bits to describe. From this perspective, the SL problem can be thought of as communication problem in which the source (unwillingly) transmits a message which is the pressure field propagating through the underwater channel. The content of this message is which grid cell contained the source, and the message is received as pressure observations at a hydrophone array. The goal of the SL algorithm is to receive this message based on the pressure observations at the array with the minimum probability of error, i.e., the minimum probability of choosing an incorrect grid cell for the source location. In MFP terms, this can be thought of as minimizing the probability of incorrectly choosing a sidelobe over the true mainlobe in the ambiguity plane.

The subsequent sections of this paper develop this approach more fully. Sec. 2 outlines an information theoretic model for the SL problem. Sec. 3 applies the Gaussian channel model to bound the mutual information between the source location and the noisy observations, and evaluates this bound for common noise models. Sec. 4 describes a simple scalar example containing several

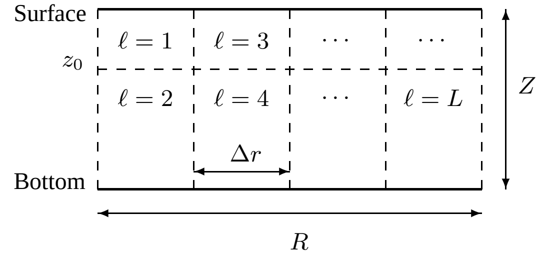

Fig. 1. Sample grid for range and depth space

Work supported by the ONR Young Investigator Program, Grant N00014-00-1-0379

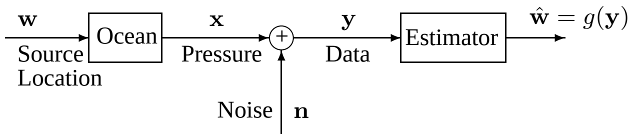

Fig. 2. Source localization model.

features of the underwater acoustic problem and illustrating why the information theory approach may be more appropriate than the CRLB for these scenarios. Sec. 5 calculates the information theoretic bound for a typical shallow water problem, and presents results from Monte Carlo simulations in this environment. Sec. 6 summarizes the advantages and disadvantages of the information theory approach in comparison to the CRLB.

2. SOURCE LOCALIZATION MODEL

Figure 2 shows a general model for the source localization problem. The unknown source location is vector random variable $\mathbf{w}$, here the range and depth of the source. The vector $\mathbf{x}(\mathbf{w})$ consists of the complex demodulated baseband pressures at the hydrophone locations for a source of unit amplitude at location $\mathbf{w}$. In underwater acoustics terms, the pressure $\mathbf{x}(\mathbf{w})$ is a vector of the Green's functions from the source location $\mathbf{w}$ to each sensor in the array, evaluated at the frequency f. The observed data is $\mathbf{y} = \mathbf{x} + \mathbf{n}$, where $\mathbf{n}$ is the complex baseband noise vector at the sensors. The SL algorithm computes an estimate $\hat{\mathbf{w}} = g(\mathbf{y})$. The estimator often incorporates information about the environment in the form of an acoustic propagation model.

As shown in Fig. 1, the set of possible source locations is partitioned into $\ell = 1, \ldots, L$ grid cells. In order to describe which grid cell contains the source, we need at least $H(\ell)$ bits of information, where $H(\ell)$ is the information entropy of the random variable ℓ [5]. The source channel coding theorem indicates that in order to estimate ℓ with arbitrarily small positive (ASP) probability of error P_e, the mutual information $I(\mathbf{w}, \hat{\mathbf{w}})$ must be greater than or equal to $H(\ell)$. Because the source channel coding theorem is an asymptotic result, receiving ℓ with ASP P_e may require block processing of a large number of messages, i.e., observing a long sequence of single sources then localizing all of them at once in batch mode. If $I(\mathbf{w}, \hat{\mathbf{w}}) \geq H(\ell)$, it is not certain that ℓ can be received with ASP P_e, but rather that some partitioning of $\mathbf{w}$ with entropy equal to $H(\ell)$ exists that can be sent with ASP P_e. This partitioning may not be contiguous and equally spaced as shown in Fig. 1. However, if $I(\mathbf{w}, \hat{\mathbf{w}}) < H(\ell)$, it can be shown that P_e is bounded away from zero [6].

Note that this scenario differs from a typical communication problem in that the user cannot completely design the code mapping from $\mathbf{w}$ to $\mathbf{x}$. The acoustics of the environment and the choice of sensor locations for the array fix the coding used to represent $\mathbf{w}$ at the sensors. All messages, i.e., source locations $\mathbf{w}$, may not be represented by equal power code words.

The mutual information $I(\mathbf{w}, \hat{\mathbf{w}})$ is difficult to compute exactly. The Data Processing Theorem (DPT) [5] allows us to put an upper bound on the mutual information between the source location and our estimate of it. The DPT demonstrates that for a Markov chain $A \leftrightarrow B \leftrightarrow C$, where A and C are conditionally independent given B, $I(A, C) \leq I(A, B)$, and $I(A, C) \leq I(B, C)$. If C is a deterministic function of B, then the requirements of a Markov chain are satisfied. Applying this result to our model produces

$$I(\mathbf{w}, \hat{\mathbf{w}}) \leq I(\mathbf{w}, \mathbf{y}), \quad (1)$$
$$I(\mathbf{w}, \mathbf{y}) \leq I(\mathbf{x}, \mathbf{y}). \quad (2)$$

Inequality (1) results because the location estimate $\hat{\mathbf{w}}$ is a deterministic function of the observed data $\mathbf{y}$. The pressure signal $\mathbf{x}$ is a deterministic function of the location $\mathbf{w}$, yielding Inequality (2). Combined, these inequalities indicate that $I(\mathbf{x}, \mathbf{y}) \geq I(\mathbf{w}, \hat{\mathbf{w}})$, the mutual information between the pressure data and the noisy observations provides an upper bound on the mutual information between the true and estimated source location. Thus, $I(\mathbf{x}, \mathbf{y}) \geq H(\ell)$ is a necessary condition to have $I(\mathbf{w}, \hat{\mathbf{w}}) \geq H(\ell)$.

For a given environment, array geometry, and distribution of source locations, it is possible to bound $I(\mathbf{x}, \mathbf{y})$. The earlier comments about $I(\mathbf{w}, \hat{\mathbf{w}})$ also apply to $I(\mathbf{x}, \mathbf{y})$. Specifically, $I(\mathbf{x}, \mathbf{y}) \geq H(\ell)$ is a necessary condition for locating the source in the correct grid cell ℓ with ASP P_e. Because this is a necessary but not sufficient condition, even if $I(\mathbf{x}, \mathbf{y}) \geq H(\ell)$, it is not guaranteed that ASP P_e can be achieved for the desired grid, but if $I(\mathbf{x}, \mathbf{y}) < H(\ell)$, it is guaranteed that ASP P_e is unachievable.

Conversely, given an upper bound on $I(\mathbf{x}, \mathbf{y})$ for a specific channel, array and source location probability density function (pdf) $p(\mathbf{w})$, it is possible to determine the largest number of grid cells with equal Δr which could be used to partition the search space while asymptotically achieving ASP P_e. Consider the grid shown in Fig. 1. Assume in the absence of outside information that that all ranges are equally likely, that the depth cells have probabilities p_{surf} and p_{sub} for surface and submerged sources respectively, and that the range and depth probabilities are independent. Let $H_z = H(p_{surf}, p_{sub})$ be the entropy of the depth pdf. Solving the necessary condition $I(\mathbf{x}, \mathbf{y}) \geq H(\ell)$ under these assumptions yields a lower bound

$$\Delta r \geq R \cdot 2^{H_z - I(\mathbf{x}, \mathbf{y})}. \quad (3)$$

Note that the Δr from this equation may not be achievable, but that any grid with a smaller Δr is guaranteed to have P_e bounded away from 0.

3. GAUSSIAN CHANNEL UPPER BOUND

It is not possible in general to write closed form analytic expressions for the pdf's of the pressure vector $\mathbf{x}$ and noisy observations $\mathbf{y}$. Thus it is usually not possible to calculate $I(\mathbf{x}, \mathbf{y})$ exactly. However, $I(\mathbf{x}, \mathbf{y})$ may be bounded from above using two common results from information theory. First, a Gaussian pdf maximizes the differential entropy $h(\mathbf{x})$ possible for any pdf $p(\mathbf{x})$ with a given covariance $\mathbf{K}_{\mathbf{xx}} = E\left(\mathbf{x}\mathbf{x}^{\mathrm{T}}\right) - E\left(\mathbf{x}\right) E\left(\mathbf{x}\right)^{\mathrm{T}}$ [5]. This is the foundation for the second result: for any additive channel with independent zero-mean Gaussian noise with covariance $\mathbf{K}_{\mathbf{nn}}$, the mutual information $I(\mathbf{x}, \mathbf{y}) \leq 0.5 \log_2(|\mathbf{K}_{\mathbf{yy}}|/|\mathbf{K}_{\mathbf{nn}}|)$, where $|\cdot|$ represents the determinant of a matrix [5]. This result holds when $\mathbf{x}, \mathbf{y}$, and $\mathbf{n}$ are real random variables. It is straightforward to show the bound becomes $I(\mathbf{x}, \mathbf{y}) \leq \log_2(|\mathbf{K}_{\mathbf{yy}}|/|\mathbf{K}_{\mathbf{nn}}|)$ for complex random variables as in the current problem. This is intuitively reasonable because with independent real and imaginary components the channel can carry twice as much information . Equality is achieved in this bound if and only if the real and imaginary parts of $\mathbf{x}$ are independent Gaussians with equal covariances.

Additional insight may be gained by considering this bound for two common noise models in underwater acoustics. Let $\mathbf{K_{xx}} = \mathbf{V_x}\Lambda_\mathbf{x}\mathbf{V_x}^\mathrm{H}$, where $(\cdot)^\mathrm{H}$ denotes the Hermitian (conjugate transpose) operator, be the eigenvalue/eigenvector decomposition for the signal covariance $\mathbf{K_{xx}}$. In a practical problem, $\Lambda_\mathbf{x}$ will have M significant eigenvalues $\lambda_{\mathbf{x}1}, \ldots, \lambda_{\mathbf{x}M}$ corresponding to the degrees of freedom in the acoustic channel. In a typical shallow water environment, this will be the number of trapped propagating modes.

The spatially white (SW) noise model assumes that $\mathbf{K_{nn}} = \sigma_\mathbf{n}^2\mathbf{I}$, with the real and imaginary parts of $\mathbf{n}$ being independent, zero-mean Gaussian random variables with equal variances $\sigma_\mathbf{n}^2/2$. Under these assumptions, the Gaussian channel upper bound on $I(\mathbf{x},\mathbf{y})$ reduces to

$$I(\mathbf{x},\mathbf{y}) \leq \sum_{m=1}^{M} \log_2\left(1 + \frac{\lambda_{\mathbf{x}m}}{\sigma_n^2}\right). \tag{4}$$

The Kuperman-Ingenito (KI) noise model [7] proposes that surface-generated noise is spatially structured. For vertical arrays in shallow water, the KI noise covariance reduces to the form $\mathbf{K_{nn}} = \Psi\Lambda_\mathbf{n}\Psi^\mathrm{H}$, where Ψ is the matrix of the trapped mode profiles sampled at the array hydrophone depths. In this model, the noise propagating in each mode is independent of the other modes. Since both $\mathbf{x}$ and $\mathbf{n}$ are propagating in the space spanned by the modes, i.e., span(Ψ), $\mathbf{V_x}$ forms an orthogonal basis for both the signal and noise subspaces in this model. If R is much larger than all of the intermodal interference distances in the channel, the modes in the signal model are essentially uncorrelated. Consequently, the same basis $\mathbf{V_x}$ decorrelates both $\mathbf{K_{xx}}$ and $\mathbf{K_{nn}}$, and the bound on the $I(\mathbf{x},\mathbf{y})$ reduces to

$$I(\mathbf{x},\mathbf{y}) \leq \sum_{m=1}^{M} \log_2\left(1 + \frac{\lambda_{\mathbf{x}m}}{\lambda_{\mathbf{n}m}}\right) \tag{5}$$

This result differs from the SW model in that the denominator is now the noise power in each mode, rather than $\sigma_\mathbf{n}^2$.

4. A SIMPLE MOTIVATING EXAMPLE

This section presents a comparison of the CRLB with the information theoretic bound derived in the previous sections for a simple scalar problem. The scalar estimation problem is

$$y = e^{j2\pi ma} + n,$$

where a is uniformly distributed on the interval $[0,1)$, m is an integer and n is a complex Gaussian random variable with variance σ_n^2. This simplified scalar problem still contains an important feature of the shallow water array SL problem: the observations y are a nonlinear, periodic (or quasi-periodic) function of the desired parameter a. The periodicity causes ambiguity in determining a from y which dominates the effect of n on estimator performance. Consequently, the CRLB will be loose, and will provide misleading conclusions about the impact of changing m or σ_n^2 on the mean squared error (MSE). The information theoretic bound will correctly predict that performance will be independent of m.

Using the formulation from [8], the Fisher information from the observed data is

$$J_D = -E_y\left\{\frac{\partial^2}{\partial a^2}\ln p(y|a)\right\} = \frac{2m^2}{\sigma_n^2}. \tag{6}$$

If a were an unknown deterministic parameter, the CRLB would be $\sigma_n^2/(2m^2)$. The a priori distribution on a random a can only increase the Fisher information, and thus the performance bound on the MSE for the random parameter case must be less than or equal to the CRLB for the related deterministic parameter problem. Since the CRLB decreases monotonically to zero as m increases, the bound on the MSE must also go to zero as m increases. If this bound is tight, the MSE should decrease as $1/m^2$ as m increases. To find the information theoretic bound, it can be shown that $\sigma_y^2 = 1 + \sigma_n^2$, and thus $I(a,y) \leq \log(\sigma_y^2/\sigma_n^2) = \log(1 + 1/\sigma_n^2)$. For a given σ_n^2, $\hat{a}$ should be able to be assigned to one of $2^{I(a,y)} = 1 + 1/\sigma_n^2$ partitions of $[0,1)$ with ASP P_e in the asymptotic limit if the partitions are properly chosen. Note that the number of partitions is independent of m.

The ML estimator for this problem is $\hat{a} = \tan^{-1} y$ [9]. When several values of a had equal likelihood, the estimator chose randomly among the candidate $\hat{a}$'s maximizing $p(y|a)$. Monte Carlo simulations were run evaluating the behavior of the ML estimator under both the MSE and P_e performance metrics. Each simulation ran 10^6 trials for given values of m and σ_n^2. Table 1 presents the results for a suite of simulations holding σ_n^2 fixed at 1/3 while varying $m = 1, 2, 4, 8$. This σ_n^2 gives $I = 2$ bits, and thus a maximum of 4 equal-width partitions on $[0,1)$. The performance under two different partitioning schemes is compared. The first, $P_{e,c}$, is for the contiguous partitioning $[\ell/4, (\ell+1)/4)$ for $\ell = 0,1,2,3$. This is the scalar analog of the contiguous grid partition shown in Fig. 1 that would be desired in SL. This performance is contrasted with the probability of error $P_{e,nc}$ for a noncontiguous partitioning such that the ℓth partition is

$$\bigcup_{k=0}^{m-1}\left[\frac{\ell}{2^{m+1}} + \frac{k}{2^{m-1}}, \frac{\ell+1}{2^{m+1}} + \frac{k}{2^{m-1}}\right),$$

for $\ell = 0,1,2,3$. This second partition is chosen such that ambiguous multiple peaks of the likelihood function for $m \geq 2$ will fall within the same cell. Note that for a uniformly distributed on $[0,1)$, both partitions have equal entropy.

The simulations show that the MSE increases with increasing m, rather than decreasing as the CRLB does. Thus, for this periodic mapping from a to y, the CRLB is not tight. In fact, as m increases the CRLB becomes more loose. The contiguous partition shows that although $I = 2$ for all m, $P_{e,c}$ also increases with increasing m. This result illustrates that $I = 2$ is a necessary but not sufficient condition to achieve the desired performance with the contiguous partition. Thus, the four contiguous partitions do not achieve the desired performance, but any equal-width partition with cells less than 0.25 wide is guaranteed not to achieve ASP P_e. The more complicated noncontiguous partition designed by exploiting the signal model demonstrates performance $P_{e,nc}$ that is independent of m. Thus, the desired contiguous partition does not achieve good performance, but another partition with equal entropy does.

The second set of Monte Carlo simulations on this model hold $m = 4$ fixed while varying σ_n^2 for different SNRs. Table 2 reports that the MSE was generally insensitive to increasing SNR, even though the CRLB decreased (based on increasing J_D in Eq. 6.) In fact, the MSE was dominated by errors due to choosing the incorrect value of $\hat{a}$ among several candidates that maximized the likelihood function, and not by the local impact of the observation noise characterized by σ_n^2. The four-celled partitions used in the first set of simulations were also used to calculate $P_{e,c}$ and $P_{e,nc}$ for this set. The desired contiguous partition demonstrated uniformly poor performance in $P_{e,c}$ across SNR, again demonstrating that having two or more bits of mutual information is a necessary, not sufficient condition, for ASP P_e. The partition matched to the signal model does show $P_{e,nc}$ decreasing as SNR increases. For appropriately chosen cell boundaries, it is less probable that the noise will perturb the observations across a cell boundary as the noise power decreases. For both the MSE and $P_{e,c}$ cases, the errors are dominated by choosing sidelobes over the correct mainlobe.

5. SHALLOW WATER EXAMPLES

This section applies the results of Sec. 3 to the typical shallow water environment shown in Fig. 3. This downwardly refracting soundspeed with a thermocline at 20 m in depth based on measurements taken in Vineyard Sound, Massachusetts (41° 07' N, 71° 02' W) on 23 August 1993. The bottom is an infinite fluid halfspace with soundspeed $c_b = 1770$ m/s and density $\rho_b = 1.8$ g/cm^3. The source is assumed to be transmitting at 100 Hz with unknown phase. Seven modes are trapped in this environment at 100 Hz. There are 33 hydrophones in a vertical line array equally spaced from 3 m to 99 m in depth. All source positions between 5 and 15 km in range are equiprobable, and surface and submerged sources are equally likely. The threshold separating surface from submerged sources is $z_0 = 20$ m. Lastly, the source is assumed to have a known amplitude. This last assumption is not realistic, but allows application of the Gaussian channel model. It is also in keeping with the spirit of this simulation, which is to examine a best-case scenario for the SL problem, with an extensive array, exact environmental knowledge, and correct assumptions about the source location pdf.

The best-case range resolution achievable in this environment is computed using the bound developed in this paper. Pressure vectors $\mathbf{x}$ were calculated every 2 m in range and every 2 m in depth over the search range using the numerical underwater acoustic simulation program OASES [10]. The same program calculated the noise covariance $\mathbf{K_{nn}}$. All pressure vectors were rotated such that the first element $\mathbf{x}_1$ was real. The resulting ensemble contains no information about the source location in absolute phase, but only in the relative phases between the signals at different hydrophone. This models the unknown phase of the source. The sample covariance $\mathbf{K_{xx}} = E_\mathbf{w}\left(\mathbf{x}(\mathbf{w})\mathbf{x}(\mathbf{w})^{\mathrm{H}}\right) - E_\mathbf{w}\left(\mathbf{x}(\mathbf{w})\right) E_\mathbf{w}\left(\mathbf{x}(\mathbf{w})\right)^{\mathrm{H}}$ was estimated, where $E_\mathbf{w}$ denotes expectation over all possible source locations $\mathbf{w}$.

Fig. 4 shows the best-case range resolution for a stationary, 100 Hz source in this scenario. The horizontal axis shows the average SNR $= 10\log_{10}(\text{trace}(\mathbf{K_{xx}})/\text{trace}(\mathbf{K_{nn}}))$ over the search space and the vertical axis plots the resulting best-case Δr for an equally spaced range grid from Eq. (3). For a given desired range resolution, this graph provides the minimum SNR necessary to achieve such resolution. The KI noise model produces a tighter resolution bound for SNR less than roughly -3 dB, above which the SW noise model gives a tighter bound. The SW noise model requires a minimum average SNR of about -6.1 dB to achieve a nominal Δr of 250 m, while the KI noise model requires a minimum SNR of -7.1 dB.

Monte Carlo simulations of 10^3 trials each were run at SNRs of 0, 3, 6 and 12 dB for this environment. Each simulation used MVDR MFP [3] to estimate the source location from the data. The inverse covariance matrix was estimated from 40 independent snapshots generated using the spatially structured noise covariance $\mathbf{K_{nn}}$ calculated for the environment by OASES. Surface and submerged sources were equally likely, and each source range was equally likely. There was no environmental or sensor location mismatch. The CRLB for this environment would be difficult to calculate, and would likely demonstrate strong positional dependence like those presented in [4]. Table 3 presents the range and depth MSEs for each simulation. The true and estimated source locations were assigned to a 64 cell grid of the form shown in Fig. 1, with $\Delta r = 325$ m and $z_0 = 20$ m. The resulting error probabilities are given as $P_{e,c}$ in Table 3. Fig. 4 shows clearly that all four SNRs simulated exceed the minimum threshold necessary for $\Delta r = 325$ m. Again, the high values of P_e in Table 3 indicate that satisfying the necessary conditions on the SNR do not guarantee adequate performance on the desired partition. The noncontiguous partition used to compute $P_{e,nc}$ in Table 3 assigns source locations to cells based on the relative phases between modes 2, 3, and 4 with mode 1. This ad hoc approach is not necessarily optimal, but is based on intuition about how the pressure field is encoding position information. The resulting $P_{e,nc}$ is less than for $P_{e,c}$ for all four SNRs examined.

6. CONCLUSION

This paper presents an alternative approach to bounding performance in the underwater source localization problem, shifting the focus from the CRLB to an information theory perspective. This new perspective provides best case performance bounds for a given environment, array geometry and source location pdf. The advantages of the new approach include algorithm independence. It is valid for biased or unbiased estimators, and is not tied to a specific estimator such as beamforming or MFP. Additionally, it is operationally motivated in its gridding of the search space, and it provides a more appropriate framework for evaluating the impact of sidelobes in low SNR scenarios. Lastly, it is more straightforward to compute than the CRLB since it does not require implementing numerical derivatives for underwater acoustic environments.

The disadvantages of this approach include that it provides only necessary and not sufficient conditions for achieving the desired performance. It does not provide a method to construct partitions achieving desired performance. Second, the bounds obtained are asymptotic and not generally achievable with realistic processing latency. Third, the source level is unrealistically assumed to be known.

There are reasons to expect that practical SL scenarios may achieve better performance than shown. Specifically, it may be possible to exploit source motion and multiple frequency components to obtain additional information about the source location, and thus better performance.

The author thanks Doug Abraham, Kristine Bell, Steve Greineder, Jim Preisig, Andy Singer, Ryuji Suzuki, John Tague, and Kathleen Wage for helpful discussions of this work.

7. REFERENCES

[1] Don H. Johnson and Dan E. Dudgeon, *Array Signal Processing: Concepts and Techniques*, Prentice Hall Signal Processing Series. Prentice Hall, Englewood Cliffs, NJ, 1993.

[2] Harry L. Van Trees, *Optimum Array Processing: Detection, Estimation, and Modulation Theory, Part IV*, John Wiley and Sons, New York, NY, 2002.

m	MSE	$P_{e,c}$	$P_{e,nc}$
1	0.0503	0.2221	0.2221
2	0.1376	0.5559	0.2211
4	0.1593	0.7504	0.2226
8	0.1659	0.7494	0.2211

Table 1. Monte Carlo results for 10^6 trials with fixed $\sigma_n^2 = 1/3$ (4.8 dB SNR) and varying m.

SNR	MSE	$P_{e,c}$	$P_{e,nc}$
4.8 dB	0.1593	0.7504	0.2226
11.8 dB	0.1578	0.7501	0.0936
20 dB	0.1569	0.7499	0.0359
40 dB	0.1641	0.7499	0.0035

Table 2. Monte Carlo results for 10^6 trials with fixed $m = 4$ and varying SNR. Both P_e measures are calculated using the same 4 partitions from Table 1

[3] A. B. Baggeroer, W. A. Kuperman, and P. N. Mikhalevsky, “Overview of matched field methods in ocean acoustics,” *IEEE Journal of Oceanic Engineering*, vol. 18, no. 4, pp. 401–424, October 1993.

[4] A. B. Baggeroer, W. A. Kuperman, and H. Schmidt, “Matched field processing: Source localization in correlated noise as an optimum parameter estimation problem,” *Journal of the Acoustical Society of America*, vol. 83, no. 2, pp. 571–587, February 1988.

[5] T. M. Cover and J. A. Thomas, *Elements of Information Theory*, Wiley Series in Telecommunications. Wiley, New York, 1991.

[6] R. G. Gallager, *Information Theory and Reliable Communication*, Wiley, New York, 1968.

[7] W. A. Kuperman and F. Ingenito, “Spatial correlation of surface generated noise in a stratified ocean,” *Journal of the Acoustical Society of America*, vol. 67, no. 6, pp. 1988–1996, June 1980.

[8] H. L. Van Trees, *Detection, Estimation, and Modulation Theory, Part I*, John Wiley and Sons, New York, 1968.

[9] Steven M. Kay, *Fundamentals of Statistical Signal Processing: Estimation Theory*, Prentice Hall, Englewood Cliffs, NJ, 1993.

[10] Henrik Schmidt, *OASES, Version 1.7 Application and Upgrade Notes*, Dept. of Ocean Engineering, Massachusetts Institute of Technology.

SNR	r MSE	z MSE	$P_{e,c}$	$P_{e,nc}$
0 dB	2.74×10^7	1.53×10^3	0.75	0.62
3 dB	2.53×10^7	1.40×10^3	0.66	0.52
6 dB	2.12×10^7	1.27×10^3	0.53	0.42
12 dB	1.38×10^7	0.85×10^2	0.33	0.27

Table 3. Monte Carlo results for 10^3 trials using MVDR MFP in the environment of Fig. 3 with 40 snapshots.

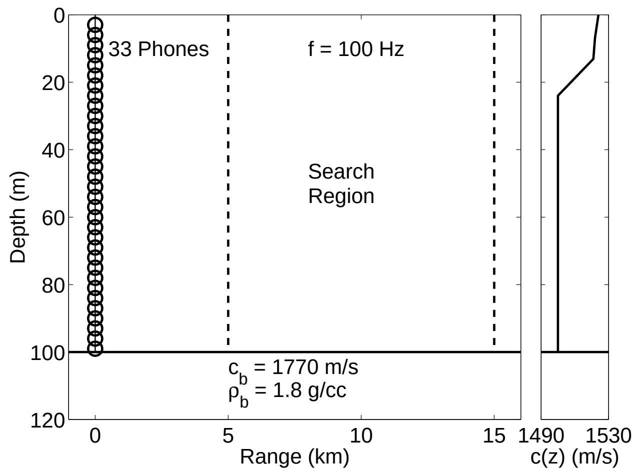

Fig. 3. Shallow water environment

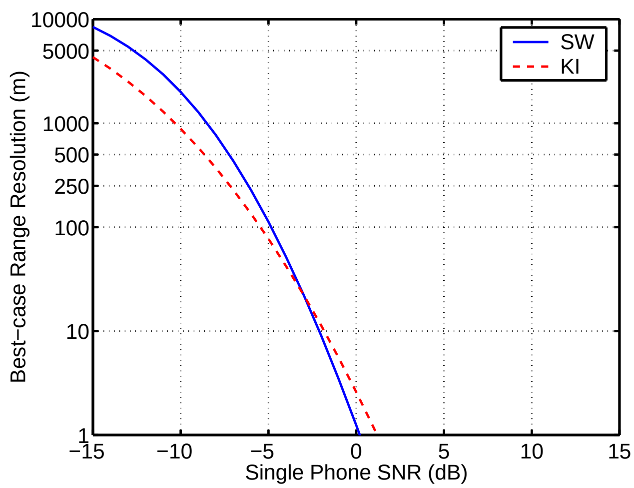

Fig. 4. Best-case range resolution vs. average SNR for both spatially white (SW) and Kuperman-Ingenito (KI) noise models. The results shown assume a stationary monochromatic ($f = 100$ Hz) source in the environment shown in Fig. 3.